


## Article

# Coastline Bathymetry Retrieval Based on the Combination of LiDAR and Remote Sensing Camera

Yicheng Liu <sup>1,2</sup>, Tong Wang <sup>1</sup>, Qiubao Hu <sup>3</sup>, Tuanchong Huang <sup>3</sup>, Anmin Zhang <sup>1,\*</sup> and Mingwei Di <sup>1,\*</sup> 

<sup>1</sup> School of Marine Science and Technology, Tianjin University, No. 92 Weijin Road, Tianjin 300072, China; liuyicheng1990s@163.com (Y.L.); wangtongmic@outlook.com (T.W.)

<sup>2</sup> Tianjin Research Institute for Water Transport Engineering, M.O.T., No. 2618, Xingang Second Road, Binhai New Area, Tianjin 300456, China

<sup>3</sup> Jiangxi Port Group Co., Ltd., No. 249, Fuhe North Road, Donghu District, Nanchang 330006, China; 1397091707@139.com (Q.H.); htcbjfu@163.com (T.H.)

\* Correspondence: tjuzhanganmin@outlook.com (A.Z.); dimingwei\_marine@tju.edu.cn (M.D.)

**Abstract:** This paper presents a Compact Integrated Water–Land Survey System (CIWS), which combines a remote sensing camera and a LiDAR module, and proposes an innovative underwater topography retrieval technique based on this system. This technique utilizes high-precision water depth points obtained from LiDAR measurements as control points, and integrating them with the grayscale values from aerial photogrammetry images to construct a bathymetry retrieval model. This model can achieve large-scale bathymetric retrieval in shallow waters. Calibration of the UAV-mounted LiDAR system was conducted using laboratory and Dongjiang Bay marine calibration fields, with the results showing a laser depth measurement accuracy of up to 10 cm. Experimental tests near Miaowan Island demonstrated the generation of high-precision 3D seabed topographic maps for the South China Sea area using LiDAR depth data and remote sensing images. The study validates the feasibility and accuracy of this integrated scanning method for producing detailed 3D seabed topography models.

**Keywords:** compact integrated water–land survey system; coastal bathymetric retrieval; LiDAR; control points; aerial imagery; ranging error calibration



**Citation:** Liu, Y.; Wang, T.; Hu, Q.; Huang, T.; Zhang, A.; Di, M. Coastline Bathymetry Retrieval Based on the Combination of LiDAR and Remote Sensing Camera. *Water* **2024**, *16*, 3135. <https://doi.org/10.3390/w16213135>

Academic Editor: Roohollah Noori

Received: 18 September 2024

Revised: 18 October 2024

Accepted: 28 October 2024

Published: 1 November 2024



**Copyright:** © 2024 by the authors. Licensee MDPI, Basel, Switzerland. This article is an open access article distributed under the terms and conditions of the Creative Commons Attribution (CC BY) license (<https://creativecommons.org/licenses/by/4.0/>).

## 1. Introduction

A coastal zone is abundant in resources such as aquaculture, wind energy, and photovoltaics. To develop and protect these marine resources, accurate measurement, surveying, and investigation of the coastal zone are essential. However, this region presents significant challenges due to its complex environment, where access from both land and sea is difficult, making fieldwork particularly demanding. Shallow water depth measurement has long been a critical and challenging aspect of coastal zone monitoring. Traditional acoustic systems for depth measurement are not only cumbersome and complicated but also inefficient when covering large areas, often requiring extended operational periods. Moreover, in nearshore or reef regions with complex and uncertain topography, the risk of vessel grounding further complicates the process [1,2]. To overcome these limitations, remote-sensing-based depth measurement and retrieval methods have gained popularity among researchers. These techniques offer a valuable complement to traditional hydrographic surveys, particularly for coastal waters [3,4].

Remote sensing-based bathymetric retrieval methods offer advantages such as a broad detection perspective and extensive measurement range, enabling large-scale bathymetric retrieval. Bathymetric retrieval models mainly include theoretical interpretation models; semi-theoretical, semi-empirical models; and statistical correlation models. Theoretical interpretation models are based on radiative transfer equations and calculate water depth by measuring optical parameters within the water [5–7]. Although theoretically rigorous,

these models are complex due to the many difficult-to-obtain optical parameters, limiting their widespread application. Semi-theoretical, semi-empirical models use the radiative attenuation characteristics of light in water, combining theoretical models with empirical parameters for bathymetric retrieval. Spitzer et al. [8] proposed a dual-stream radiative model for depth and substrate composition retrieval based on solar radiation reflection spectra. Lyzenga et al. [5] proposed a logarithmic bathymetric retrieval model based on band-ratio-processing methods. Subsequently, Lyzenga et al. [9] improved the single-band model by developing a method to extract water depth information using passive multispectral scanner data and evaluated the retrieval results, exploring the limitations of the model. Benny and Dawson [10] used contour lines to invert large areas' water depth information by combining attenuation coefficients with limited measured depths. Su [11] proposed a geographically adaptive model, dividing regions based on substrate types and selecting parameters accordingly for bathymetric retrieval. Rangzan et al. [12] introduced a hybrid method based on principal component analysis and image fusion, as well as new algorithms combining particle swarm optimization and genetic algorithms, significantly improving depth measurement accuracy in high turbidity conditions. Statistical correlation models obtain depth data by establishing relationships between remote sensing image spectral values and measured depths. Ceyhun et al. [13] used neural network bathymetric retrieval models with Terra satellite's ASTER and Quickbird satellite images for bathymetric retrieval in a Turkish bay. Ai et al. [14] proposed a convolutional neural network method, leveraging local spatial correlations in image pixels and combining different spectral bands for depth extraction. These methods can achieve high accuracy but often struggle to obtain precise depth measurements in unknown areas, making them more feasible in known regions for algorithm assessment.

Airborne LiDAR bathymetry leverages the relatively low attenuation of blue–green light, specifically within the 470 to 580 nm wavelength range, to accurately measure underwater topography in shallow waters. This technology offers high measurement accuracy, safety, efficiency, and the ability to perform integrated coastline measurements, providing a new solution to issues like incomplete data in shallow regions and serving as an effective complement to acoustic depth sounding in these areas. Over the decades, airborne LiDAR bathymetry systems have undergone several generations of updates. In 1968, Hickman and Hog, in the United States, developed the world's first laser depth-measurement system. Subsequently, NASA successfully developed the Airborne LiDAR Bathymetry System (ALB) and later introduced the Airborne Oceanographic LiDAR (AOL) system with high-speed data recording and scanning capabilities [15]. In the 1980s, advancements in high-speed data recording and scanning functionalities, along with the integration of positioning and attitude determination technologies, led to the development of representative products such as the Hawk Eye series and LADS series [16]. In the 21st century, airborne LiDAR bathymetry systems have reached a commercial stage, with prominent manufacturers including Velodyne LiDAR (USA), Hexagon AB (Sweden), Riegl (Austria), and Teledyn Optech (Canada). The Shanghai Institute of Optics and Fine Mechanics, Chinese Academy of Sciences, has developed three generations of airborne bathymetry systems, with the third-generation Mapper5000 dual-frequency system successfully completing experiments in the South China Sea. Additionally, organizations such as the Naval Hydrographic and Oceanographic Office, the First Institute of Oceanography, Ministry of Natural Resources, Guilin University of Technology, Shenzhen University, and Shandong University of Science and Technology have also engaged in developing airborne LiDAR bathymetry equipment [17]. In 2017, the China Natural Resources Airborne Geophysical Remote Sensing Center procured the CZMIL Nova II system and conducted experiments to analyze its application potential in China's coastal regions [18]. However, the effective depth range of airborne LiDAR systems is highly dependent on the water quality, and most existing laser sensors are both large and power-intensive. They typically require mounting on manned aircraft or large unmanned aerial vehicles, increasing both the application threshold and measurement costs.

To overcome the limitations of traditional remote sensing images and LiDAR systems and to harness their complementary strengths for shallow-water depth measurement along coastline, this study introduces a Compact Integrated Water–Land Survey (CIWS) device. Weighing just 6 kg, the system can be easily carried by UAV. The core sensors of the system include a camera and a low-power LiDAR system, enabling the simultaneous acquisition of remote sensing imagery and LiDAR depth data. Firstly, the accuracy of the LiDAR system's measurements is calibrated to achieve high-precision depth values. Subsequently, a remote sensing bathymetric retrieval algorithm based on aerial imagery is proposed, which uses LiDAR-acquired depth values as control points to achieve bathymetric retrieval near the coastline. Finally, the integrated device was tested near Miaowan Island in the South China Sea, successfully measuring underwater terrain and performing large-scale bathymetry retrieval in the region.

The Compact Integrated Water–Land Survey System presented in this paper combines remote sensing imagery and LiDAR, offering advantages over traditional methods. The device is smaller and lighter, making it easy to carry and mount on small drones, which enhances its portability and practicality. Traditional laser bathymetry systems rely solely on laser data, whereas this new system integrates both a camera and LiDAR, enabling the simultaneous acquisition of remote sensing imagery and laser bathymetry data. By proposing a remote-sensing-based water depth inversion algorithm for aerial imagery, the system utilizes LiDAR bathymetric data as control points to achieve accurate, large-scale water depth inversion. The advantage of this multisensor fusion provides a new technological path for amphibious surveying, addressing the limitations of previous single-technology approaches in shallow water measurements.

## 2. Compact Integrated Water–Land Survey System

This study utilizes a self-designed device, the Compact Integrated Water–Land Survey (CIWS) system, primarily comprising a visible light camera, camera controller, laser emitter, laser reflector, laser receiving lens, laser receiving detector, laser signal processor, industrial computer, and data storage units for both laser and image data, along with the overall structural and mounting components, as illustrated in Figure 1. The design integrates a visible light camera and laser in a shared optical path to address the issues of multisystem fusion and miniaturization, with the device weighing only 6 kg, suitable for UAV platforms. A 532 nm pulsed laser, a critical element of the integrated remote sensing system, emits a high-repetition-frequency (10 Hz) laser from the airborne platform to the sea surface, measuring distances to the sea surface and seabed to capture underwater topography. In line with conventional photogrammetry requirements, which dictate a photo overlap of 60–65% along the flight path and 20–30% across adjacent flight lines, as well as considering typical UAV speeds of 8 to 12 m/s, a 50-megapixel camera was selected. The camera features 3.76  $\mu\text{m}$  pixels, a CMOS sensor with a physical size of 30.8  $\times$  24 mm, a resolution of 8200  $\times$  6380 pixels, and a 21 mm focal length lens.

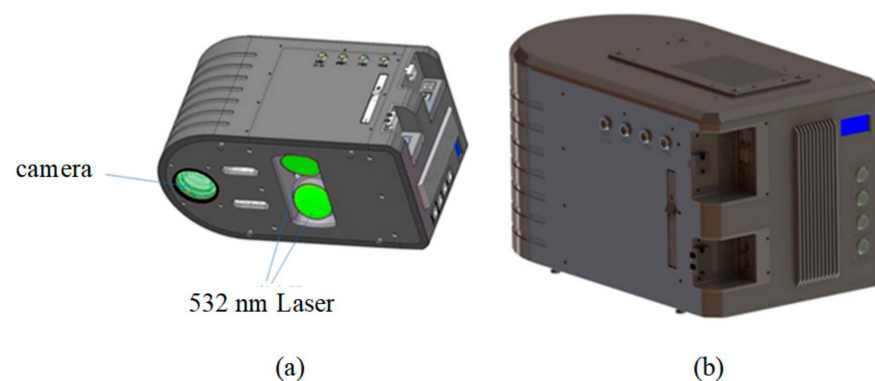


**Figure 1.** Appearance of the CIWS system: (a) 3D model; (b) actual photograph.

### 3. Calibration of Airborne LiDAR Depth Measurement Precision

#### 3.1. Laboratory Calibration

Before performing bathymetric retrieval, it is necessary to calibrate the LiDAR system to ensure its depth measurement accuracy. This study used LiDAR from the CIWS system, corresponding to the laboratory distance measurement device. The field test in the pool is shown in Figure 2, and the experimental principle is illustrated in Figure 3. A 3D printed object with a height of 0.1 m was created to simulate different water depths. The 3D printed object was placed directly below the laser, with different water depth values tested 100 times. The results, shown in Table 1, indicate that the LiDAR can achieve centimeter-level precision.

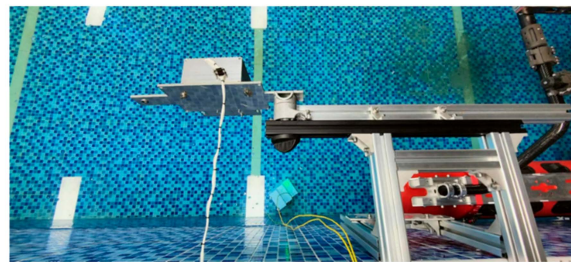


**Figure 2.** Simulation of different water depths based on 3D printed models.

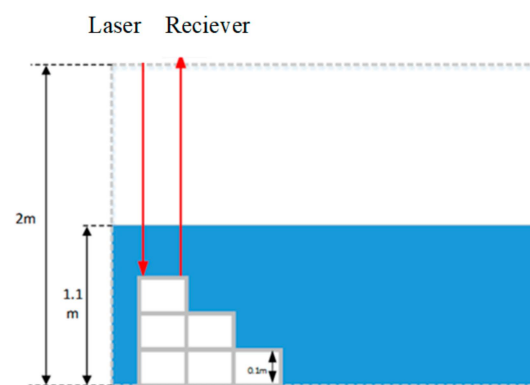


**Figure 3.** Schematic diagram of the distance measurement error calibration experiment.

**Table 1.** Laboratory calibration results of the LiDAR system (unit: m).

Group	Actual Distance	Maximum Measurement Error	Average Measurement Error
(a)	2.000	0.051	0.035
(b)	1.900	0.043	0.029
(c)	1.800	0.061	0.034
(d)	1.700	0.049	0.037

Since the accuracy of the laser spot position affects the measurement precision, which in turn impacts the accuracy of bathymetry retrieval, calibrating the LiDAR is of great significance for improving the final precision. From the calibration results in Table 1, it can be seen that the distance measurement accuracy of the laser remains relatively stable at different distances. The maximum measurement error ranges from 0.043 m to 0.061 m, while the average measurement error is between 0.029 m and 0.037 m. Overall, the distance measurement accuracy of the laser meets the requirements for high-precision water depth measurement, serving as the foundation for subsequent bathymetry retrieval.

#### 3.2. Airborne LiDAR Bathymetry Data Processing

The raw data collected by the airborne LiDAR bathymetry system primarily include POS data, base station data, code wheel data, waveform data, and auxiliary data (such as

imagery and video data). After undergoing data preprocessing, waveform data processing, error correction, and point cloud data processing, water depth data along the flight path is ultimately obtained. The overall process of airborne laser bathymetry data is illustrated in Figure 4.

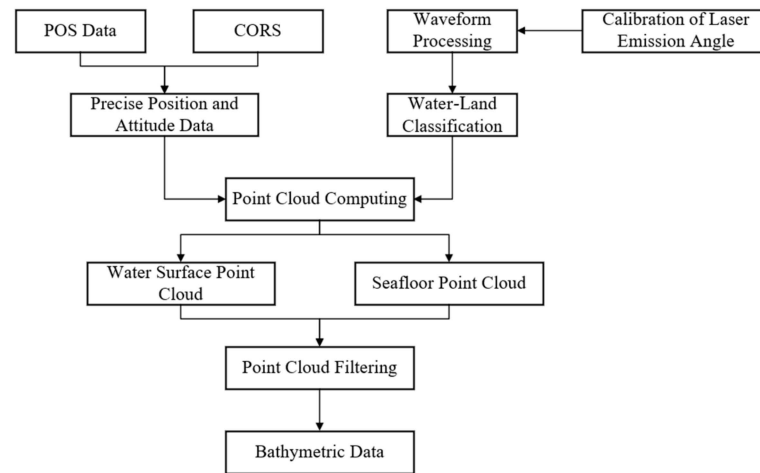


**Figure 4.** Processing flow of airborne LiDAR bathymetry data.

Data preprocessing mainly includes POS data processing and calibration of positioning parameters. In this study, POS uses Real-Time Kinematic (RTK) technology to compute the initial position at the laser pulse emission moment. The attitude changes of the flight platform are then obtained from IMU data. By applying a Kalman filter and iterative feedback error control, the spatial position at the time of laser pulse emission, as well as the roll, pitch, and yaw angles of the platform, are determined. The calibration of the installation parameters primarily involves determining the position and tilt angles of the LiDAR sensor relative to the platform's center, which is typically performed during factory calibration before equipment delivery. Waveform data processing is conducted on the industrial computer of the integrated device, involving waveform denoising, deconvolution, peak detection, and numerical simulation methods. Because of the differences in laser pulse propagation characteristics in the water and air, waveform data are also used for water–land classification, laying the foundation for subsequent data processing. After obtaining the propagation time of the laser points, error mitigation is essential to ensure the accuracy of the bathymetric. Errors mainly include positioning errors, equipment installation errors, and water surface refraction errors, which can be reduced through high-precision positioning algorithms, laboratory calibration, and modeling [19–21].

### 3.3. Calibration of LiDAR Bathymetry Accuracy in Coastal Area

In Section 3.1, LiDAR calibration was conducted in a pool. However, the shallow, clear water and calm surface conditions differ significantly from real ocean environments. Additionally, during laboratory calibration, only errors of the laser ranging system were present. In airborne LiDAR bathymetry, determining seabed depth introduces additional errors beyond LiDAR ranging, such as GNSS positioning errors, UAV attitude errors, and installation errors from various instruments. Even with modeling to mitigate these errors, they cannot be completely eliminated, and these residual errors ultimately affect the accuracy of depth measurements, leading to increased bathymetric error [22].

Therefore, it is necessary to calibrate the LiDAR bathymetry accuracy of the system under real oceanic conditions. Calibration tests were conducted at the Dongjiang Bay calibration site in Tianjin, as shown in Figure 5. Initially, a multibeam bathymetric system mounted on an Unmanned Surface Vessel (USV) Dolphin-1 was used to map the 3D topography of the target water area, providing a reference seabed terrain for the UAV-based LiDAR bathymetry calibration.

The Dolphin-1, equipped with the Norbit iWBMS system, was used to survey the bathymetry of the calibration field, as shown in Figure 6. The Norbit iWBMS is a high-resolution, integrated multibeam echo sounding system that incorporates the POS MV (Position and Orientation Systems for Marine Vessels) WaveMaster inertial navigation system, eliminating the need for additional inertial navigation equipment. In previous calibration studies, the processed multibeam data demonstrated a depth accuracy of better than 5 cm within a 10 m depth range [23]. Although the bathymetric accuracy is lower than that of LiDAR, its ability to provide full 3D coverage of the seafloor makes it an ideal reference for calibrating airborne LiDAR bathymetry. The processed 3D multibeam seafloor image is shown in Figure 7, with the maximum depth in the surveyed area reaching approximately 10 m.



Figure 5. Calibration field at Dongjiang Bay.

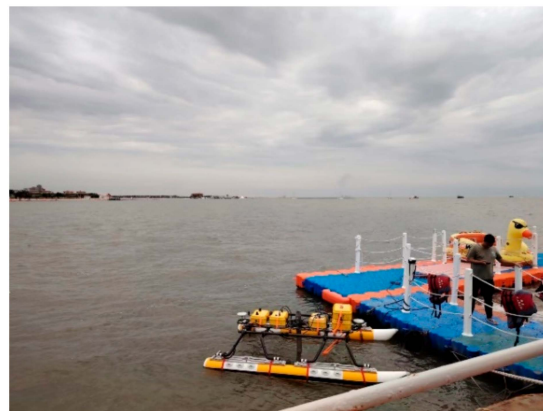


Figure 6. Multibeam bathymetric survey experiment with the Norbit iWBMS and Dolphin-1 USV.

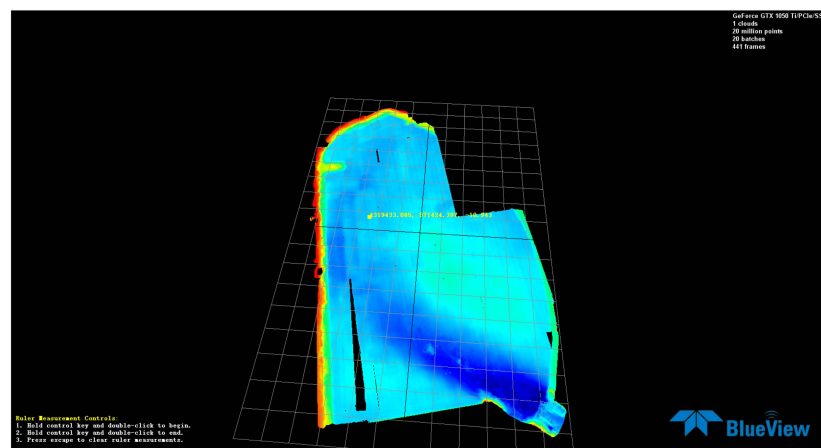
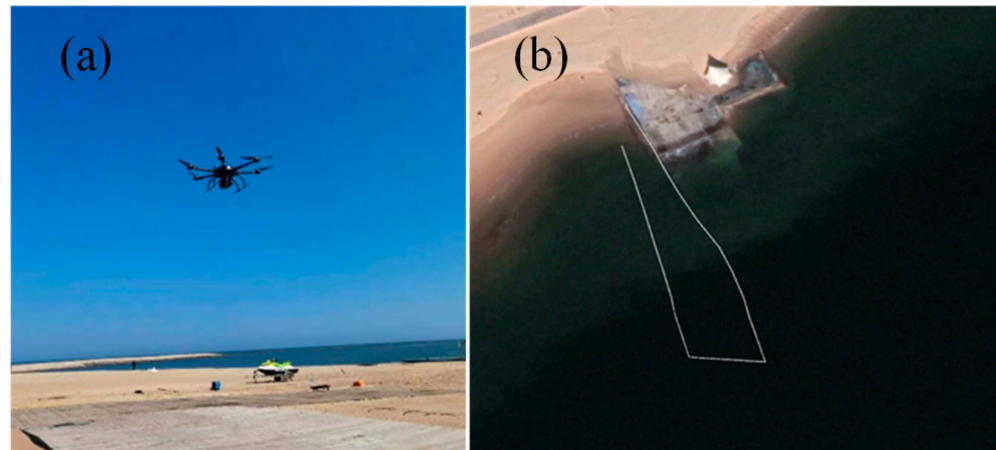


Figure 7. Seafloor topography of Dongjiang Bay, obtained from multibeam data.

The CIWS was mounted on a hexacopter, as shown in Figure 8. Figure 8a shows the hexacopter with the CIWS system during takeoff, and Figure 8b shows the flight trajectory of the hexacopter. Because of the relatively turbid water quality in the Dongjiang Bay, calibration tests were conducted exclusively in nearshore areas.



**Figure 8.** Calibration experiment of the CIWS: (a) hexacopter UAV equipped with the CIWS system; (b) flight trajectory.

To verify the accuracy of the laser bathymetry in the CIWS, multibeam bathymetric points were interpolated onto the LiDAR points using the Inverse-Distance-Weighting (IDW) method. The formula is expressed as follows:

$$\tilde{z}(x_l, y_l) = \frac{\sum_{i=1}^N w_i z_i}{\sum_{i=1}^N w_i} \quad (1)$$

$$w_i = \frac{1}{d_i^p} \quad (2)$$

In this formula,  $w_i$  denotes the weight of the multibeam depth point  $i$ ,  $d_i$  represents the distance from point  $i$  to the LiDAR footprint point,  $p$  is an adjustable parameter typically set to 2 or 3,  $(x_l, y_l)$  are the coordinates of the LiDAR footprint point, and  $\tilde{z}$  is the depth obtained through inverse-distance-weighting interpolation.

The Root Mean Square Error (RMSE) was used to measure the accuracy of the laser bathymetry, and the results show that the laser bathymetry accuracy of the CIWS can reach 11.3 cm.

We conducted a statistical analysis of the absolute error of the LiDAR depth measurement as a function of depth, as shown in Figure 9. It can be observed that the error gradually increases with depth, particularly after 9 m, where the error increases significantly.

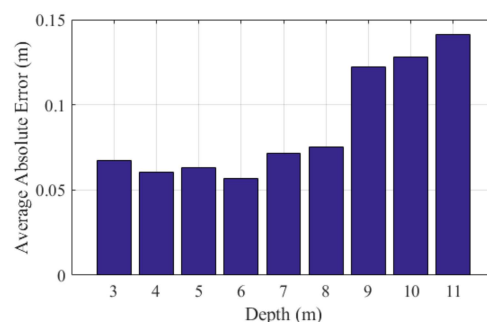


**Figure 9.** Average error at different depths.

#### 4. Depth Measurement and Retrieval Algorithm Using CIWS

The high-precision water depth values obtained from the water surface and seabed are one-dimensional strips using the LiDAR system, which are insufficient for creating extensive, high-precision, and three-dimensional seabed topographies. Therefore, we used high-precision water depth points, obtained from the LiDAR, as control points, combined with the grayscale values from aerial images, to construct a bathymetric retrieval model. This model was then applied to achieve large-area, high-precision seabed topography mapping. This section primarily focuses on the construction of the bathymetric retrieval model and the production of large-area, high-precision, and three-dimensional seabed topography.

##### 4.1. Bathymetric Retrieval Model Construction

Lyzenga et al. [9] proposed a method that uses the difference in radiance between shallow and deep water pixels in an image for a logarithmic-linear transformation. This method interprets the exponential attenuation of visible light in water using a single band, and it has been further extended to dual-band and multiband linear models. The specific algorithm formula is as follows:

$$z = a_0 + \sum_{i=1}^N a_i \ln(R_i - (R_\infty)_i) \quad (3)$$

In this formula, where  $a_0$  and  $a_i$  are constant coefficients,  $N$  is the number of bands involved in the retrieval,  $R_i$  is the radiance value of the band, and  $(R_\infty)_i$  is the radiance value of the optical deep water pixel in a neighboring shallow water area. It is usually denoted as  $X_i = \ln(R_i - (R_\infty)_i)$ , and when combined with the panchromatic band images from aerial photogrammetry, the bathymetric retrieval model can be constructed as follows:

$$z = a_0 + a_1 \ln\left(R_{pancolour} - (R_\infty)_{pancolour}\right) \quad (4)$$

High-precision water depths extracted from LiDAR point clouds are input into the bathymetric retrieval model to solve for the parameters  $a_0$  and  $a_1$ , thus completing the construction of the bathymetric retrieval model.

##### 4.2. Accuracy Analysis of Bathymetric Retrieval Algorithms

To verify the reliability of the method, remote-sensing-image data from GeoEye-1, a high-resolution multispectral satellite, were used for the experiment, as shown in Figure 10a. The image was taken on 18 February 2013, based on the WGS-84 coordinate system and the Universal Transverse Mercator projection, with a spatial resolution of 2 m. It includes four bands: blue, green, red, and near-infrared. This multispectral image data were collected under cloud-free conditions and in good weather. The water depth data for the region are from a composite product of LiDAR and multibeam bathymetry data collected in May 2016.

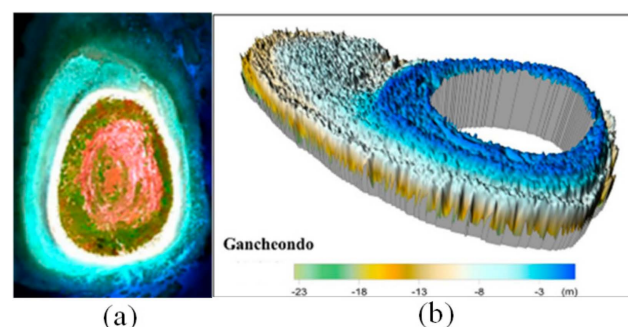


**Figure 10.** High-precision 3D seabed topography retrieval of the Ganchcondo water area based on remote sensing images. (a) high-resolution multispectral satellite (b) 3D model of the underwater terrain.



Based on the method described, 2000 measured points were selected from the remote sensing image, with 400 points used as training data to fit the regression model parameters  $a_0$  and  $a_1$ . The remaining 1600 depth points served as validation for assessing model accuracy. The bathymetric retrieval model parameters were then calculated using Equation (4) for this region, and the bathymetric retrieval model was applied to aerial photogrammetry images. By using the pixel values of the images and performing band operations, a 3D seabed topography with the same spatial resolution as the images was obtained.

After this, a triangular mesh method was used for visualizing the underwater topography. Specifically, the depth information was triangulated to create a corresponding triangular mesh model, which was then rendered to generate a 3D model of the underwater terrain. The retrieval results are shown in Figure 10b.

Figure 11 compares the model-derived depths with the actual measured depths. It is evident that the correlation coefficient between the inverted and measured depths is 0.97, with an RMSE of 1.07 m.

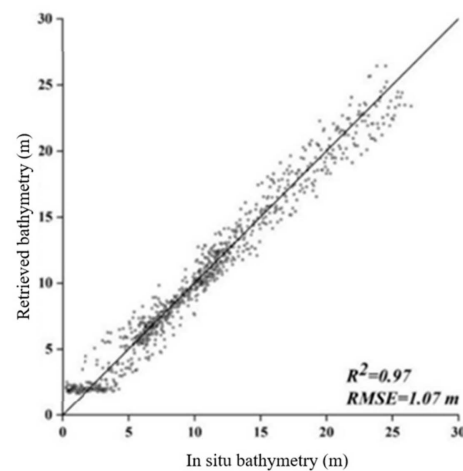


**Figure 11.** Comparison between simulated model water depths and measured water depths.

#### 4.3. Bathymetric Retrieval Using CIWS Systems

This study conducted experimental tests at Miaowan Island in Zhuhai. Miaowan Island is located in the South China Sea, south of the Pacific Ocean, and 48.8 km north of Hong Kong. The island features unique wind-eroded coastal landforms and a complex, scattered reef system, creating an ideal environment for marine life. However, this complex terrain poses challenges for traditional depth measurement methods. Given the area's distance from the mainland, using conventional shipborne depth-sounding equipment is both time-consuming and labor-intensive, with the measurement accuracy significantly affected by sea conditions. Therefore, the study employed a hexacopter equipped with the CIWS system to enhance the accuracy and efficiency of the depth measurements in this region.

In April 2024, an integrated system mounted on a hexacopter was used to perform CIWS in the primary marine areas surrounding Miaowan Island. The hexacopter flew along predetermined paths, as shown in Figure 12, capturing LiDAR point cloud data and aerial remote sensing imagery covering the entire study area; some of these aerial images are shown in Figure 13. The high resolution of the LiDAR allowed for accurate depth data acquisition even in the complex seabed terrain, laying the foundation for subsequent bathymetric retrieval.

After completing the image stitching, high-precision water depth information obtained from LiDAR point cloud data were combined with the stitched remote sensing imagery; then, the bathymetric retrieval model was constructed using the method described in Section 4.1. A quantitative relationship between the radiance value and water depth was

established based on the water depth measurements obtained from the airborne LiDAR point clouds.



**Figure 12.** Integrated measurement experiment on Miaowan Island.



**Figure 13.** Aerial imagery data acquired by the CIWS system.

Using the constructed bathymetric retrieval model, a triangular mesh model was employed to perform bathymetric retrieval over a large area near Miaowan Island. By combining LiDAR data with remote sensing image data, the system successfully sampled the study area, performed bathymetric retrieval, and produced a water depth map of the waters around Miaowan Island, as shown in Figure 14.

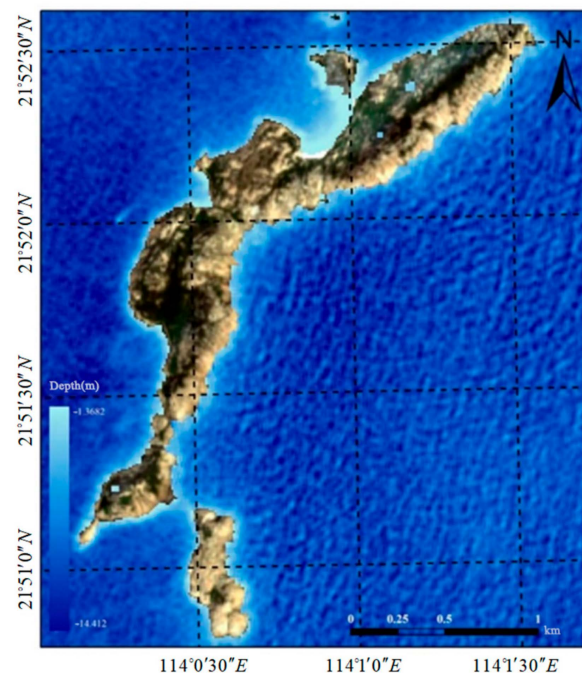


**Figure 14.** Bathymetric retrieval results of the coastal area of water at Near Miaowan Island.

## 5. Conclusions and Future Outlook

This study developed a CIWS device, incorporating both a visible light camera and an airborne LiDAR system. By designing a common optical path for both the visible light and laser, the issue of multisystem integration and miniaturization was addressed, enabling precise and rapid water depth measurement in shallow areas such as islands and reefs.

To ensure the accuracy of the water depth measurements, calibration experiments were conducted for the airborne LiDAR system. Initially, calibration was performed in a laboratory water tank, where 3D printed objects simulated different seabed depths. The results indicate that the underwater depth measurement accuracy of the LiDAR could reach centimeter-level precision. Subsequently, to verify its accuracy in shallow water areas, calibration tests were conducted at the Dongjiang Bay calibration site in Tianjin. Based on the depth measurements from a multibeam sonar system, the results showed that the RMSE of the CIWS was 11.3 cm.

A method was proposed to use the high-precision water depth points obtained from LiDAR as control points, combined with the radiance values from aerial photogrammetry images, to construct a bathymetric retrieval model. Using existing GeoEye-1 high-resolution multispectral remote sensing images and depth data, the feasibility of this method was verified. The correlation coefficient between the inverted water depth and the measured water depth reached 0.97, with a Root Mean Square Error (RMSE) of 1.07 m, demonstrating the high reliability and accuracy of this method, particularly in shallow water and clear water environments where LiDAR bathymetry can provide precise data.

The depth measurement capability of LiDAR bathymetry systems is primarily influenced by the turbidity of the water. Generally, the clearer the seawater and the lower the turbidity, the more easily the laser can penetrate the water, resulting in a greater effective depth range. LiDAR bathymetry systems perform optimally in sea states of level three or below, which indicates that in relatively calm conditions, the laser beam can penetrate the water surface smoothly and conduct effective underwater terrain surveys [24]. As sea conditions worsen, waves, foam, and other disturbances may interfere with the transmission of the laser signal, reducing the accuracy and range of the measurements.

In order to improve the accuracy of bathymetry retrieval, the following issues need to be considered in future work. When using lasers for depth sounding, the continuous undulations of the ocean surface affected the accuracy of the laser measurements. In this

study, a multiframe filtering method was employed, assuming that wave fluctuations are random. By performing multiple measurements and averaging the results, more accurate depth information was obtained. In the future, we will continue to study wave-related parameters to reduce the impact of waves on laser measurement results. At the same time, the multiframe filtering method has certain limitations. When the angle of the waves is too large, some signals cannot be received properly, resulting in lower filtering accuracy in such cases.

With the development of machine learning, methods combining nonlinear regression models established through machine learning with bathymetric retrieval have become widely used and have been a hotspot in recent years. In the future, we will incorporate neural network models into the retrieval process to achieve higher precision remote sensing bathymetric retrieval based on high-precision LIDR bathymetric data.

**Author Contributions:** Conceptualization, methodology, software, and writing—original draft preparation, Y.L.; conceptualization, methodology, validation, funding acquisition, and writing—review and editing, M.D.; data curation, methodology, investigation, supervision, and project administration, A.Z.; investigation, software, resources, writing—original draft preparation, writing—review and editing, T.W.; formal analysis, Q.H.; investigation, T.H. All authors have read and agreed to the published version of the manuscript.

**Funding:** This research was funded by the National Key Research and Development Program of China (Grant No. 2022YFB3207404), Tianjin Research Innovation Project for Postgraduate Students (Grant No. 2022BKY088), Tianjin University Graduate School of Arts and Sciences Outstanding Innovation Award Program (Grant No. B1-2021-009), and Department of Transportation Science and Technology Project, Jiangxi Province (Grant No. 2023C0010).

**Data Availability Statement:** Data will be made available upon request.

**Conflicts of Interest:** Although two of the authors are affiliated with Jiangxi Port Group Co., Ltd., this article has no conflict of interest with the company. The authors declare no conflicts of interest.

## References

1. Zhi, H.; Siwabessy, J.; Nichol, S.L.; Brooke, B.P. Predictive mapping of seabed substrata using high-resolution multibeam sonar data: A case study from a shelf with complex geomorphology. *Mar. Geol.* **2014**, *357*, 37–52. [[CrossRef](#)]
2. Zhao, J.; Ouyang, Y.; Wang, A. Status and development tendency for seafloor terrain measurement technology. *Acta Geod. Cartogr. Sin.* **2017**, *46*, 1786. (In Chinese)
3. Li, M.; Zhang, A.; Zhang, D.; Di, M.; Liu, Q. Automatic Sounding Generalization Maintaining the Characteristics of Submarine Topography. *IEEE J. Sel. Top. Appl. Earth Obs. Remote Sens.* **2021**, *14*, 10278–10286. [[CrossRef](#)]
4. Chen, B.; Yang, Y.; Xu, D.; Huang, E. A dual band algorithm for shallow water depth retrieval from high spatial resolution imagery with no ground truth. *ISPRS J. Photogramm. Remote Sens.* **2019**, *151*, 1–13. [[CrossRef](#)]
5. Lyzenga, D.R. Passive remote sensing techniques for mapping water depth and bottom features. *Appl. Opt.* **1978**, *17*, 379–383. [[CrossRef](#)]
6. Lee, Z.; Carder, K.L.; Steward, R.G.; Peacock, T.G.; Davis, C.O.; Mueller, J.L. Remote sensing reflectance and inherent optical properties of oceanic waters derived from above-water measurements. In Proceedings of the SPIE 2963, Ocean Optics XIII, Halifax, NS, Canada, 22–25 October 1996; SPIE: Bellingham, WA, USA, 1997; pp. 160–166.
7. Ma, Y.; Zhang, J.; Zhang, J.Y.; Zhang, Z.; Wang, J. Progress in shallow water depth mapping from optical remote sensing. *Adv. Mar. Sci.* **2018**, *36*, 331–351.
8. Spitzer, D.; Dirks, R.W.J. Bottom Influence on the Reflectance of the Sea. *Int. J. Remote Sens.* **1987**, *8*, 279–308. [[CrossRef](#)]
9. Lyzenga, D. Remote Sensing of Bottom Reflectance and Water Attenuation Parameters in Shallow Water Using Aircraft and Landsat Data. *Int. J. Remote Sens.* **1981**, *2*, 71–82. [[CrossRef](#)]
10. Benny, A.H.; Dawson, G.J. Satellite imagery as an aid to bathymetric charting in the Red Sea. *Cart. J* **1983**, *20*, 5–16. [[CrossRef](#)]
11. Su, H.; Liu, H.; Wang, L.; Filippi, A.M.; Heyman, W.D.; Beck, R.A. Geographically adaptive inversion model for improving bathymetric retrieval from satellite multispectral imagery. *IEEE Trans. Geosci. Remote Sens.* **2013**, *52*, 465–476. [[CrossRef](#)]
12. Rangzan, K.; Kabolizadeh, M.; Karimi, D. Optimized water depth retrieval using satellite imageries based on novel algorithms. *Earth Sci. Inf.* **2022**, *15*, 37–55. [[CrossRef](#)]
13. Ceyhun, Ö.; Yalçın, A. Remote sensing of water depths in shallow waters via artificial neural networks. *Estuar. Coast. Shelf Sci.* **2010**, *89*, 89–96. [[CrossRef](#)]
14. Ai, B.; Wen, Z.; Wang, Z.; Wang, R.; Su, D.; Li, C.; Yang, F. Convolutional neural network to retrieve water depth in marine shallow water area from remote sensing images. *IEEE J. Sel. Top. Appl. Earth Obs. Remote Sens.* **2020**, *13*, 2888–2898. [[CrossRef](#)]

15. Muirhead, K.; Cracknell, A.P. Airborne lidar bathymetry. *Int. J. Remote Sens.* **1986**, *7*, 597–614. [[CrossRef](#)]
16. Liu, Y.; Guo, K.; He, X.; Xu, W.; Feng, Y. Research progress of airborne laser bathymetry technology. *Geomat. Inf. Sci. Wuhan Univ.* **2017**, *42*, 1185–1194. (In Chinese)
17. Cui, Z.; Xu, W.; Liu, Y.; Guo, Y.; Meng, X.; Jiang, Z. Current status of the acquisition and processing of airborne laser sounding data. *Remote Sens. Nat. Resour.* **2023**, *35*, 1–9. (In Chinese)
18. Li, Q.; Wang, J.; Han, Y.; Gao, Z.; Zhang, Y.; Jin, D. Potential evaluation of China's coastal airborne LiDAR bathymetry based on CZMIL Nova. *Remote Sens. Land Resour.* **2020**, *32*, 184–190. (In Chinese)
19. Ye, X.; Zhang, C.; Wang, A. Analysis of the airborne laser scanning bathymetry errors. *J. Geomat. Sci. Technol.* **2008**, *25*, 400–402. (In Chinese)
20. Yang, F.; Su, D.; Ma, Y.; Feng, C.; Yang, A.; Wang, M. Refraction correction of airborne LiDAR bathymetry based on sea surface profile and ray tracing. *IEEE Trans. Geosci. Remote Sens.* **2017**, *55*, 6141–6149. [[CrossRef](#)]
21. Di, M.; Zhang, A.; Guo, B.; Zhang, J.; Liu, R.; Li, M. Evaluation of real-time PPP-based tide measurement using IGS real-time service. *Sensors* **2020**, *20*, 2968. [[CrossRef](#)]
22. Di, M.; Guo, B.; Ren, J.; Li, M.; Chen, X.; Zhang, A. Sea surface height measurements using a low-cost GNSS buoy with multiple GNSS receivers. *Ocean Eng.* **2023**, *277*, 114362. [[CrossRef](#)]
23. Cao, G.; Zhou, X.; Ling, J.; Xu, H. NORBIT iWBMS Application of multi-beam echo sounding system in monitoring Sanjiang river channel in Ningbo City. *Zhejiang Hydrotech.* **2021**, *49*, 87–90. (In Chinese)
24. Wang, H.; Yin, Y.; Jing, Q.; Cong, L. Estimation of the Berthing Parameter of Unmanned Surface Vessels Based on 3D LiDAR. *J. Syst. Simul.* **2024**, *36*, 1737–1748.

**Disclaimer/Publisher's Note:** The statements, opinions and data contained in all publications are solely those of the individual author(s) and contributor(s) and not of MDPI and/or the editor(s). MDPI and/or the editor(s) disclaim responsibility for any injury to people or property resulting from any ideas, methods, instructions or products referred to in the content.